O-annulation to Polycyclic Aromatic Hydrocarbons: a Tale of Optoelectronic Properties from Five- to Seven-Members Rings

Luka Đorđević,[†‡] Domenico Milano,[‡] Nicola Demitri[§] and Davide Bonifazi[†,#,*]

[†] School of Chemistry, Cardiff University, Main Building, Park Place, Cardiff CF10 3AT, United Kingdom.

[‡] Department of Chemical and Pharmaceutical Sciences, Trieste; University of Trieste, via Licio Giorgieri 1, Trieste 34127, Italy.

[§] Elettra − Sincrotrone Trieste, S.S. 14 Km 163.5 in Area Science Park, 34149 Basovizza, Trieste, Italy.

[#] Institute of Organic Chemistry, Faculty of Chemistry, University of Vienna, Währinger Str. 38
1090, Vienna, Austria.

Supporting Information Placeholder

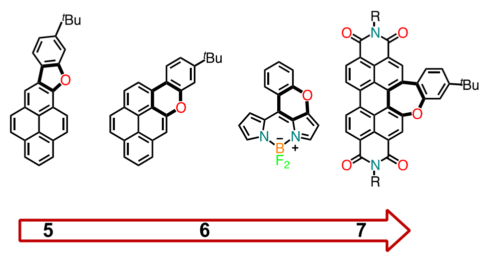

ABSTRACT: We take advantage of the *Pummerer* oxidative annulation reaction to extend PAHs through the formation of an intramolecular C−O bond with a suitable phenol substituent. Depending on the peripheral topology of the PAH precursor (*e.g.*, pyrene, boron-dipyrromethene or perylene bisimide) five-, six- and seven-member O-containing rings could be obtained. The effect of the O-annulation on the optoelectronic properties was studied by various methods, with the pyrano-annulated pyrene and BODIPY derivatives depicting quantitative emission quantum yields.

The π-extension of polycyclic aromatic hydrocarbons (PAHs) is a powerful approach in the chemical toolbox for tailoring properties of organic molecules and materials.[1] Amid the synthetic approaches, fusing and replacing benzene rings with heterocycles have emerged as attractive routes to tailor the band gaps, redox properties, self-assembly properties, aromaticity, and chemical stability of PAHs.[2] Traditionally, PAHs have been synthesized through multistep protocols building on polyarylated precursors, followed by a planarization reaction to obtain the fused aromatic scaffold. Representative examples of this approach are the hexa-*peri*-hexabenzocoronene (HBC) and its heteroatom-doped analogues.[3] Another approach comprises of the annulative π-extension (APEX) reactions of PAHs, which can be selective at their bay- or k-regions.[4] A recent example accomplishes APEX on thiophene, benzofuran and indole derivatives, using a Pd-catalyzed dual C−H annulation with π-extensive dibenzosiloles and dibenzogermoles.[5] Another general strategy includes the (benz)annulation reactions of *o*-ethynylbiaryls precursors.[6] Ethynylbiaryls can also be combined with anthranil, through Au-catalyzed π-extension, for preparing N-doped PAHs.[7] π-Extension through alkyne annulation has recently attracted attention for the synthesis of non-planar PAHs. Examples includes PAHs prepared through electrocatalysis with accessible boronic acids,[8] as well as Rh-catalysis for synthesizing N- and S-doubly doped, and cationic thiazoloquinolinium scaffolds.[9]

Compared to the five- or six-membered N- or S-containing heteroaromatics, O-based extended π-system are less common, with the 7-member rings being very rare, *i.e.* oxepin,[10] and five-member furans[11] the most popular rings. The two main synthetic approaches include intramolecular carbon−heteroatom bond formation of biaryl alcohols[12] and intramolecular C−C bond formation of biaryl ethers.[13] As depicted in Scheme 1, the preparation of five- and six-membered O-annulated PAHs were successfully reported through, for example, base-promoted cyclization of *o*-ethynylphenol substructures,[14] acid-mediated cyclization of alkynes with alcohols or ketones,[15] acid-mediated condensation between ketones and phenols,[16] Friedel-Crafts reactions, (followed by cyclodehydrogenation),[17] Claisen-condensation between arylaldehydes and naphthols (followed by oxidation),[18] cross-condensation between hydroquinone and arylaldehyde derivatives for the simultaneous formation of C−C and C−O bonds,[19] and Rh-catalyzed C−H activation/annulations of arylaldehydes with diaryl alkynes.[20] In this context, our group has recently applied the *Pummerer* oxidative cyclisation[21] as planarization reaction for the synthesis of O-doped nanographenes[22] and molecular ribbons with various peripheral topologies (armchair and zig-zag),[23] as well as for the cyclization of 2,2′-binaphthol derivatives for the preparation of π-extended and imide-based *peri*-xanthenoxanthenes (PXX).[24] Similar Cu-catalyzed C−H/C−O cyclization of 2,2′-binaphthol derivatives was recently used to develop chiral PXXs, exhibiting intense circularly polarized luminescence both in solution and the solid state.[25]

Scheme 1. Common synthetic approaches towards O-annulated PAHs

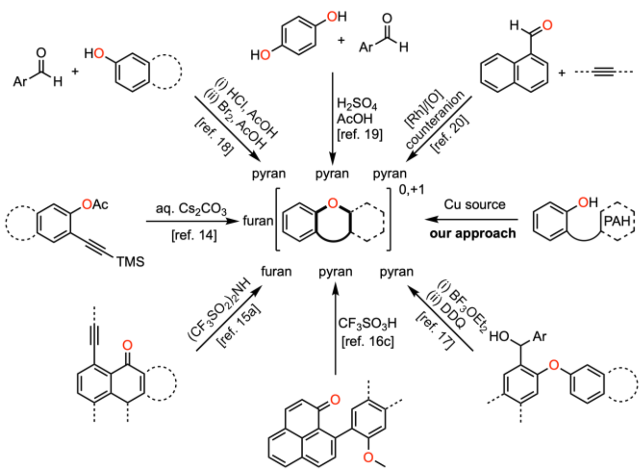

Now, we report on the π-extension through O-fusion on different classes of PAHs. Specifically, we used the Cu-mediated ring closure of relevant phenol precursors to obtain five-, six- and seven-member O-containing heterocycles. Different ring sizes were accessible through the appropriate choice of substituted PAHs, which include pyrene,[26] boron-dipyrromethene (BODIPY)[27] and perylene bisimide (PBI).[28] The synthetic routes are depicted in Scheme 2.

To obtain furan-bearing $\mathbf{1}^{fused}$ (Scheme 2, *i*-*iv*), pyrene was first borylated, through Ir-catalyzed C−H activation,[29] in 2-position.[29] Suzuki-Miyaura Pd-catalyzed cross-coupling with 5-*tert*-butyl-2-iodoanisole, afforded anisole-substituted pyrene $\mathbf{1}^{OMe}$. After demethylation with BBr_3, annulation of phenol $\mathbf{1}^{OH}$ with CuI and PivOH in DMSO gave furan derivative $\mathbf{1}^{fused}$ in fair yield. For pyran-embedded heteroarene $\mathbf{2}^{fused}$, regioselective bromination of pyrene with NBS and cross-coupling with the relevant boronic acid, led to anisole derivative $\mathbf{2}^{OMe}$ (Scheme 2, *v*-*vii*). Demethylation and C−O ring closure (with CuO in boiling nitrobenzene) gave product $\mathbf{2}^{fused}$ in excellent yield.

For the BODIPY derivative, it was possible to obtain the phenol-substituted boron-dipyrromethene precursor $\mathbf{3}^{OH}$ through TFA-catalyzed condensation of salicylaldehyde and 2,5-dimethylpyrrole, followed by DDQ oxidation to dipyrromethene and its treatment with BF_3 in the presence of Et_3N (Scheme 2, *vii*-*x*i). Molecule $\mathbf{3}^{OH}$ was successfully converted into $\mathbf{3}^{fused}$ in excellent yield, using $Cu(OAc)_2$, Cs_2CO_3 and PivOH in DMSO. BODIPY derivative $\mathbf{3}^{OH}$ was also benzylated to $\mathbf{3}^{OBn}$ for recording reference electrochemical data.

At last, molecule $\mathbf{4}^{fused}$ annulated at the bay region with an oxepin ring was prepared (Scheme 2, *xii*-*xvi*). In the synthetic strategy, perylene bisanhydride was converted into the relevant PBI with 3-aminopentane (in molten imidazole), followed by bromination with Br_2. Subsequent Pd-catalyzed Suzuki cross coupling and deprotection with BBr_3 of the corresponding anisole, gave phenol-bearing PBI precursor $\mathbf{4}^{OH}$. Finally, $\mathbf{4}^{OH}$ was converted into $\mathbf{4}^{fused}$, using $Cu(OAc)_2$, Cs_2CO_3 and PivOH in DMSO in an excellent yield. The structure of $\mathbf{4}^{fused}$ was confirmed by bidimensional NMR investigations (Figures S52-S54), and excluded the presence of any arene-oxide tautomer.[10b]

Scheme 2. Synthesis of O-annulated PAHs[a]

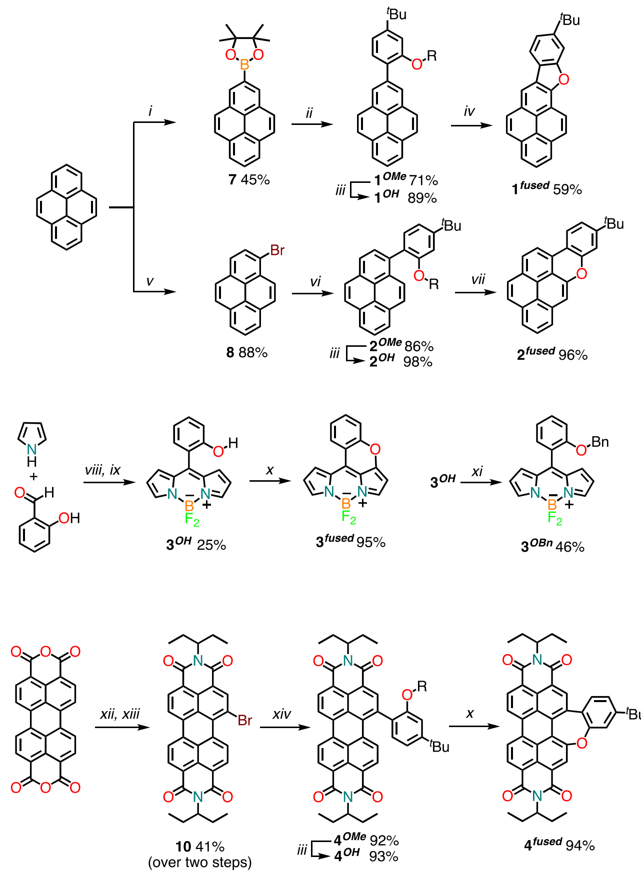

[a]Reagents and conditions: *i*) [Ir(μ-OMe)cod]$_2$, dtbpy, B$_2$pin$_2$, hexane, N_2, 80 °C; *ii*) 5-*tert*-butyl-2-iodoanisole, [Pd(PPh$_3$)$_4$], Na_2CO_3, toluene/H_2O, N_2, 120 °C; *iii*) BBr_3, CH_2Cl_2, N_2, 0 °C → r.t.; *iv*) CuI, PivOH, DMSO, 140 °C; *v*) NBS, CH_2Cl_2, r.t.; *vi*) (4-*tert*-butyl-2-methoxyphenyl)boronic acid, [Pd(PPh$_3$)$_4$], Na_2CO_3, toluene/H_2O, N_2, 120 °C; *vii*) CuO, $PhNO_2$, 240 °C; *viii*) CF_3COOH; *ix*) step 1) DDQ, CH_2Cl_2, Ar, rt; step 2) Et_3N, BF_3OEt_2, CH_2Cl_2, Ar, rt; *x*) $Cu(OAc)_2$, Cs_2CO_3, PivOH, DMSO, 140 °C; *xi*) BnBr, K_2CO_3, DMF, N_2, 70 °C; *xii*) 3-aminopentane, imidazole, N_2, 160 °C; *xiii*) Br_2, CH_2Cl_2, N_2, rt; *xiv*) 6, [Pd(PPh$_3$)$_4$], K_2CO_3, dioxane/H_2O, N_2, 100 °C.

Single crystals for X-ray diffraction were obtained for compounds $\mathbf{1}^{fused}$, $\mathbf{2}^{fused}$ and $\mathbf{3}^{fused}$ (Figure 1 and ESI Section 6). For molecule $\mathbf{1}^{fused}$, two different monoclinic crystalline phases were found (α, β). The compounds crystallize in centrosymmetric space groups with one (α,β-$\mathbf{1}^{fused}$, $\mathbf{2}^{fused}$) or two ($\mathbf{3}^{fused}$) crystallographically independent molecules. In all crystals, the aromatic cores are flat (R.M.S.D. of atoms from their mean plane are: 0.06(5) Å for α-$\mathbf{1}^{fused}$, 0.09(7) Å for β-$\mathbf{1}^{fused}$ and 0.03(3) Å for $\mathbf{2}^{fused}$, and 0.05(3) Å for $\mathbf{3}^{fused}$). Crystal packing of molecules α-$\mathbf{1}^{fused}$ and $\mathbf{2}^{fused}$ (Figures 1b$_1$ and 1d) show the presence of dimers linked by crystallographic inversion centers with π···π pairing ($d_{\pi\cdots\pi}$ 3.36(9) Å and 3.30(3) Å in $\mathbf{2}^{fused}$ and α-$\mathbf{1}^{fused}$, respectively). On the other hand, in phase β the molecules of $\mathbf{1}^{fused}$ lack significant π···π stacking contacts, preferring a herringbone arrangement governed by C−H···π interactions (Figure 1b$_2$). Finally, molecule $\mathbf{3}^{fused}$ arranges in π···π stacked pillars, with average interplanar distances between the aromatic cores of 3.38(10) Å (Figure 1f).

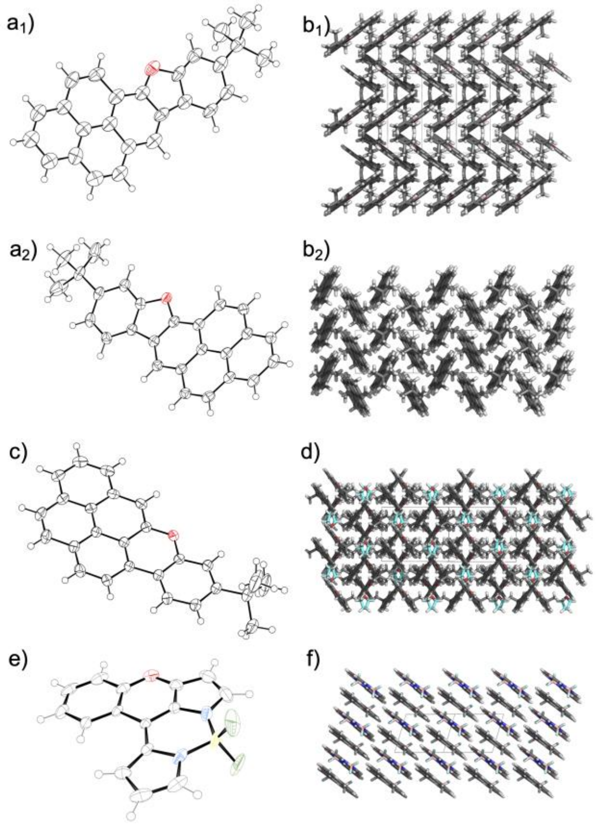

Figure 1. X-ray crystal structures of α,β-**1**^{fused}, **2**^{fused} and **3**^{fused}. Left: ellipsoids representation of X-ray structure (50% probability). Right: crystal packing; b1) view along the [401] crystallographic direction; b2) view along [501] crystallographic direction; d) View along [301] crystallographic direction (solvent molecules, THF, are shown with cyan sticks); f) View along [0-13] crystallographic direction. Atom colors: red O, gray C, yellow B, green, F.

Final compounds, along with their precursors, were characterized and their photophysical, electrochemical and computational data are summarized in Table 1 (see also ESI, Sections 3-5). From the Table, it is apparent that the O-annulation impacted the optoelectronic properties, with the extent of the effect depending on the type of the O-ring as well as the structure of the precursor chromophore/luminophore. For instance, furan-embedded **1**^{fused} exhibits red-shifted UV-Vis absorption and emission profiles (λ_{max} = 399 nm and λ_{em} = 401 nm, respectively), along with a stronger emission (Φ_{em} = 33%) if compared to anisole-pyrene **1**^{OMe} (λ_{max} = 339 nm and λ_{em} = 396 nm, with Φ_{em} = 4%). The O-annulation reaction yielding pyrenes **1**^{fused} and **2**^{fused} is accompanied also by a narrowing of the Stokes shift, compared to anisole-substituted pyrenes **1**^{OMe} and **2**^{OMe}, from 57 nm and 39 nm to 2 nm and 17 nm, respectively. Previously reported benzoheterocycle-fused pyrenes, pyrenebenzo[*b*]phosphole and -benzo[*b*]silole, showed λ_{max} = 414 (λ_{em} = 414 nm) and 354 nm (λ_{em} = 406 nm), with Φ_{em} = 30 and 4%, respectively.[30] Similarly, pyrenebenzo[*b*]thiophene showed absorption and emission maxima at λ_{max} = 338 and λ_{em} = 373 nm with Φ_{em} = 25%.[31] On the other hand, pyrano-fused heteroarene **2**^{fused} showed a stronger bathochromic shift in the absorption (λ_{max} = 433 nm) and emission (λ_{em} = 450 nm) profiles with the fluorescence quantum yield value exceptionally reaching unity (Φ_{em} = 100%). Previously reported thiopyran-fused pyrene[31] showed a similar lowest electronic transition (λ_{max} = 433 nm), but a wider Stokes' shift (λ_{em} = 480 nm) and a significantly lower Φ_{em} value (60%). In the case of boron-dipyrromethene **3**^{fused} (Figure 2a), however, the pyrano annulation resulted in a blue-shifted absorption of the optical properties and emission profiles (λ_{max} = 472 nm and λ_{em} = 489 nm) when compared to **3**^{OBn} (λ_{max} = 505 nm and λ_{em} = 522 nm), with quantative emission quantum yield (Φ_{em} = quantitative). Mayer bond order analysis for molecules **3**^{OH} and **3**^{fused} (Figure 2b) suggests that the pyranyl annulation perturbates the aromatic character of the boron-dipyrromethene skeleton, reducing the degree of π-conjugation. Similar analyses and observations were reported for BODIPYs bearing with electron donating groups, with the rings being less aromatic.[32]

Table 1. Photophysical, electrochemical and computational data of compounds reported herein

Cpd.	Photophysical^{a}					Electrochemical^{d}					Calc.^{g}
	λ_{max} [nm]	$E_{00}{}^{b}$ [eV]	$\lambda_{em,max}$ [nm]	$\Phi_{em}{}^{c}$ [%]	τ_{em} [ns]	$E_{ox,1}$ [V]	$E_{red,1}$ [V]	E_{HOMO} [eV]	E_{LUMO} [eV]	E_{gap} [eV]	E_{gap} [eV]
1^{OMe}	339	3.13	396	4	11.7	+0.85	−2.28^{e}	−5.65	−2.52	3.13	3.41
1^{fused}	399	3.09	401	33	7.3	+0.76	−2.33^{e}	−5.56	−2.47	3.09	3.26
2^{OMe}	345	3.23	384	25	16.7	+0.68	−2.55^{e}	−5.48	−2.25	3.23	3.41
2^{fused}	433	2.76	450	quant.	4.5	+0.44	−2.32^{e}	−5.24	−2.48	2.76	2.86
3^{OH}	505	2.38	522	24	2.8	+1.06^{f}	−1.36^{f}	−5.86	−3.44	2.42	2.67
3^{fused}	472	2.54	489	quant.	5.7	+1.14	−1.36	−5.94	−3.44	2.50	2.75
4^{OMe}	530	2.14	617	20	1.6	+1.08	−1.15	−5.88	−3.65	2.23	2.20
4^{fused}	538	2.20	611	4	6.0	+1.10	−1.08	−5.90	−3.72	2.18	2.14

^{a}Spectra were measured in CH_2Cl_2 (spectroscopic grade) at rt. ^{b}Calculated optical gap as E_{00} = 1240/λ_{em}. ^{c}Relative fluorescence quantum yields measured using either Quinine sulfate, Coumarin 153 or Rhodamine 6G as references. ^{d}Electrochemical data obtained from differential pulse voltammetry experiments in anhydrous CH_2Cl_2, containing 0.1 M $^{n}Bu_4PF_6$ using glassy carbon working electrode, Pt wire counter-electrode and Ag wire reference electrode. All potentials are referenced versus the Fc^{+}/Fc couple used as internal standard. HOMO and LUMO energy levels were approximated using the equations HOMO = −(4.80 + $E_{ox,1}$) and LUMO = −(4.80 + $E_{red,1}$). ^{e}Estimated as $E_{red,1}$ = $E_{ox,1}$ + E_{00}, since no reduction peaks were observed. ^{f}Measured using benzylated derivative 3^{OBn}. ^{g}Calculated from TD-DFT calculations, performed at the CAM-B3LYP/6-31G(d,p) level of theory.

As observed for pyrene derivative **2**^{fused}, the dramatic enhancement of the emission quantum yield (Φ_{em} = quantitative) is attributed to the pyranyl ring that, restricting the rotational degrees of freedom, disfavors any non-radiative deactivation of the excited state.[33]

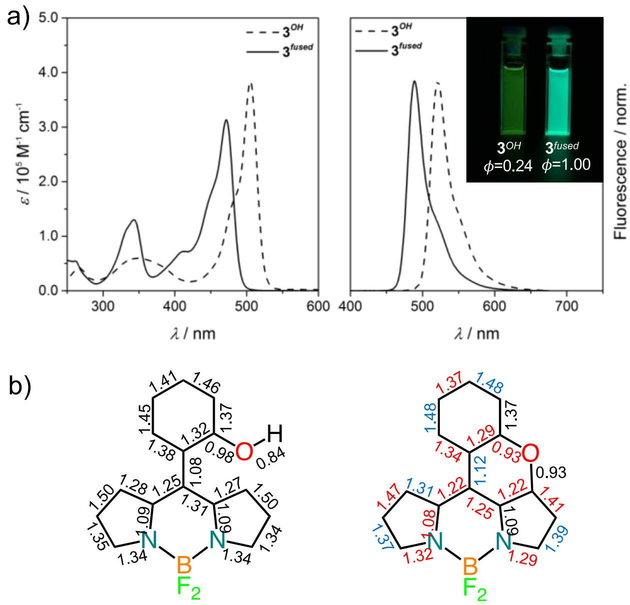

Figure 2. a) Absorption (left) and emission (right) spectra for BODIPY derivatives **3**^{OH} and **3**^{fused} in CH_2Cl_2 (inset: solutions upon irradiation with a hand-held UV lamp). b) Mayer bond order analysis for the two optimized structures (red and blue values show a decrease and increase in bond order values, respectively).

For the annulated PBI derivative, the presence of the oxepin ring in **4**^{fused} caused minor shifts to the absorption and emission spectra (λ_{max} = 538 nm and λ_{em} = 611 nm for **4**^{fused} compared to λ_{max} = 530 nm and λ_{em} = 617 nm for **4**^{OMe}) and a notable decrease of the emission quantum yield (from 20% to 4%). Considering the increase of +5.6° of the core-twist in the O-annulated PBI derivative deriving from the shallow envelope structure of the oxepin substructure (Figure S20), one could hypothesize that the decrease of the singlet emission intensity is accompanied by an increase of the population of the triplet excited state.[34] This phenomenon is triggered by an enhancement of the intersystem crossing following a perturbation of the singlet-triplet energy gap.[34] As no phosphorescence signal was detected either at rt or in frozen medium for both PBI derivatives, we indirectly measured the triplet generation by studying the photosensitization of $^1O_2$ in a cycloaddition reaction. Thus, we performed the oxidation of $^1O_2$-acceptor 9,10-dimethylanthracene (DMA) in air-equilibrated CH_2Cl_2 using either **4**^{OMe} or **4**^{fused} as photosensitizers, and monitored the formation of 9,10-endoperoxianthracene (Figure S5). As clearly appears from the inset of Figure S5, the oxygenation of DMA is faster in the presence of **4**^{OMe} than with **4**^{fused}. These observations suggest that, in contrast to the pyranyl ring, the oxepin ring has a detrimental effect on the singlet radiative properties as well as on the triplet population. We conjectured that the non-radiative deactivation is caused by a rapid inversion of the envelop-like conformation of the oxepin ring.

CV and DPV electrochemical investigations (Table 1, ESI section 4) suggest that, in the case of the pyrene derivatives, both **1**^{fused} and **2**^{fused} feature lower oxidation potentials if compared to precursors **1**^{OMe} and **2**^{OMe} ($\Delta E_{ox,1}$ = 90 and 240 mV, respectively, where $\Delta E_{ox,1} = E_{ox,1}{}^{fused} - E_{ox,1}{}^{precursor}$). As far as the reductive processes are concerned, the reduction of **1**^{fused} is cathodically shifted of 50 mV when compared to **1**^{OMe}, whereas that of **2**^{fused} is anodically shifted of 230 mV (−2.32 V *vs* Fc^+/Fc) with respect to that of **2**^{OMe}. This results in E_{gap} values for both **1**^{fused} and **2**^{fused} that are lower (ΔE_{gap} = 40 and 470 meV) than those of their precursors, with the strongest shrinking effect observed with the pyranyl derivative, in full agreement with the optical data. As far as **3**^{fused} is concerned, the reduction potential is virtually the same as that of **3**^{OBn}, whereas the oxidation process unexpectedly occurs at a slightly higher potential ($\Delta E_{ox,1}$ = 80 mV). These observations suggest the presence of a destabilization effect of the O-annulation on the first oxidative event. In agreement with the blue-shift observed in the absorption profile, these electrochemical data indicate that the widening of the electrochemical bandgap is likely caused by an energy lowering of the HOMO level. This behavior contrasts to recent reports describing widening of molecular bandgap in *meso*,*β*-heteroaryl-fused BODIPYs caused by the raising of the LUMO energy level.[35] At last, a 50 meV shrinking of the electrochemical bandgap was observed when passing from **4**^{OMe} to **4**^{fused}, in contrast to the optical investigations, which suggested a 60 meV blue shift of the lowest energy electronic transition.

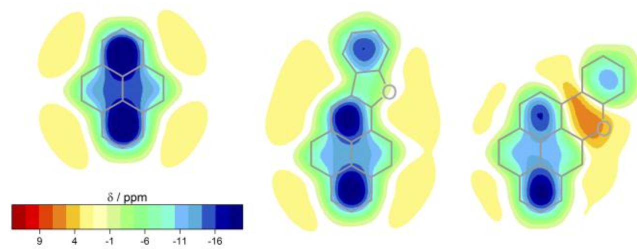

Figure 3. NICS$_{\pi zz}$-XY-scan for pyrene, **1**^{fused} and **2**^{fused}.

We have also performed theoretical calculation in order to gain a deeper insight into different heteroatom extended PAHs. After optimization of the structures, time-dependent (TD)-DFT calculations (CAM-B3LYP/6-31G**)[36] reproduced fairly well the experimental UV-Vis spectra (ESI, Figure S21-23). Nucleus-Independent Chemical Shifts (NICS)[37] were used as a criterion to access aromaticity in the planar **1**^{fused} and **2**^{fused} molecules (Figure 3 and ESI). The new formed furan ring is slightly aromatic and does not influence the aromaticity of the pyrene ring. Previously reported five-member ring benzoheterocycle-fused pyrenes, pyrene-benzo[*b*]phosphole and -benzo[*b*]silole derivatives, on the other hand, were showed to be slightly anti-aromatic and non-aromatic, respectively.[30]

In summary, we have decorated three classes of PAHs (pyrene, boron-dipyrromethene and perylene bisimide) with phenol substituents. Then, we applied the *Pummerer* oxidative cyclization for the intramolecular formation of C−O bond, which lead to the formation of O-embedded five-, six- and seven-member rings. The annulations led to substantial changes in the photophysical and electrochemical properties, compared to the parent compounds. While annulation with the pyranyl ring depicts the strongest bathochromic shifts with the emission yields reaching quantitative values, the oxepin annulation has a detrimental effect on the emission properties.

ASSOCIATED CONTENT

Supporting Information

Supporting Information contains synthetic protocols and characterizations, photophysical data, electrochemical data, crystal structures and computational details (PDF). The Supporting Information is available free of charge on the ACS Publications website.

AUTHOR INFORMATION

Corresponding Author

* bonifazid@cardiff.ac.uk; davide.bonifazi@univie.ac.at

Author Contributions

The manuscript was written through contributions of all authors. All authors have given approval to the final version of the manuscript.

Notes

Any additional relevant notes should be placed here.

ACKNOWLEDGMENTS

D.B. gratefully acknowledges the EU through the ERC Starting Grant "COLORLANDS" and MC-RISE "INFUSION" projects, the MIUR through the FIRB ("SUPRACARBON", contract n° RBFR10DAK6), and the School of Chemistry at Cardiff University for financial support. We thank Andrea Fermi and Tommaso Battisti (Cardiff University) for the lifetime measurements and the attempts to measure any phosphoresce signals and the $^1O_2$-oxidation experiment of DMA.

REFERENCES

(1) a) Chen, L.; Hernandez, Y.; Feng, X.; Müllen, K., From Nanographene and Graphene Nanoribbons to Graphene Sheets: Chemical Synthesis. *Angew. Chem. Int. Ed.* **2012,** *51*, 7640-7654; b) Narita, A.; Wang, X. Y.; Feng, X.; Müllen, K., New advances in nanographene chemistry. *Chem. Soc. Rev.* **2015,** *44*, 6616-6643; c) Segawa, Y.; Ito, H.; Itami, K., Structurally uniform and atomically precise carbon nanostructures. *Nat. Rev. Mat.* **2016,** *1*, 15002.

(2) a) Hirai, M.; Tanaka, N.; Sakai, M.; Yamaguchi, S., Structurally Constrained Boron-, Nitrogen-, Silicon-, and Phosphorus-Centered Polycyclic π-Conjugated Systems. *Chem. Rev.* **2019,** *119*, 8291-8331; b) Stępień, M.; Gońka, E.; Żyła, M.; Sprutta, N., Heterocyclic Nanographenes and Other Polycyclic Heteroaromatic Compounds: Synthetic Routes, Properties, and Applications. *Chem. Rev.* **2017,** *117*, 3479-3716; c) Szűcs, R.; Bouit, P.-A.; Nyulászi, L.; Hissler, M., Phosphorus-Containing Polycyclic Aromatic Hydrocarbons. *ChemPhysChem* **2017**, *18*, 2618 –2630.

(3) Wang, X. Y.; Yao, X.; Narita, A.; Mullen, K., Heteroatom-Doped Nanographenes with Structural Precision. *Acc. Chem. Res.* **2019,** *52*, 2491-2505.

(4) Ito, H.; Segawa, Y.; Murakami, K.; Itami, K., Polycyclic Arene Synthesis by Annulative π-Extension. *J. Am. Chem. Soc.* **2019,** *141*, 3-10.

(5) Ozaki, K.; Matsuoka, W.; Ito, H.; Itami, K., Annulative π-Extension (APEX) of Heteroarenes with Dibenzosiloles and Dibenzogermoles by Palladium/o-Chloranil Catalysis. *Org. Lett.* **2017,** *19*, 1930-1933.

(6) Senese, A. D.; Chalifoux, W. A., Nanographene and Graphene Nanoribbon Synthesis via Alkyne Benzannulations. *Molecules* **2018,** *24*, 118.

(7) Zeng, Z.; Jin, H.; Sekine, K.; Rudolph, M.; Rominger, F.; Hashmi, A. S. K., Gold-Catalyzed Regiospecific C-H Annulation of o-Ethynylbiaryls with Anthranils: π-Extension by Ring-Expansion En Route to N-Doped PAHs. *Angew. Chem. Int. Ed.* **2018,** *57*, 6935-6939.

(8) Kong, W. J.; Finger, L. H.; Oliveira, J. C. A.; Ackermann, L., Rhodaelectrocatalysis for Annulative C-H Activation: Polycyclic Aromatic Hydrocarbons through Versatile Double Electrocatalysis. *Angew. Chem. Int. Ed.* **2019,** *58*, 6342-6346.

(9) Dutta, C.; Sainaba, A. B.; Choudhury, J., Annulating thiazolium cations via a direct double C-H activation strategy: Rh-N,S-heterocyclic carbene is the key. *Chem. Commun.* **2019,** *55*, 854-857.

(10) a) Vogel, E.; Schubart, R.; Böll, W. A., Synthesis of an Oxepin Derivative. *Angew. Chem. Int. Ed.* **1964,** *3*, 510-510; b) Boyd, D.; Jerina, D., Arene Oxides-Oxepins. In *Small Ring Heterocycles, Part 3*, Hassner, A., Ed. Wiley & Sons Ltd: Arene Oxides-Oxepins, 1985; Vol. 42, p 198.

(11) a) Gidron, O.; Diskin-Posner, Y.; Bendikov, M., α-Oligofurans. *J. Am. Chem. Soc.* **2010,** *132*, 2148-2150; b) Gidron, O.; Dadvand, A.; Wei-Hsin Sun, E.; Chung, I.; Shimon, L. J. W.; Bendikov, M.; Perepichka, D. F., Oligofuran-containing molecules for organic electronics. *J. Mater. Chem. C* **2013,** *1*; c) Gidron, O.; Bendikov, M., α-Oligofurans: an emerging class of conjugated oligomers for organic electronics. *Angew. Chem. Int. Ed.* **2014,** *53*, 2546-2555.

(12) a) Rossignon, A.; Bonifazi, D., O-Annulation Leading to Five-, Six-, and Seven-Membered Cyclic Diaryl Ethers Involving C–H Cleavage. *Synthesis* **2019,** *51*, 3588-3599; b) Elbert, S. M.; Reinschmidt, M.; Baumgärtner, K.; Rominger, F.; Mastalerz, M., Benzopyrano-Fused N-Heterocyclic Polyaromatics. *Eur. J. Org. Chem.* **2018,** *2018*, 532-536; c) Chen, D.; Zhu, D.; Lin, G.; Du, M.; Shi, D.; Peng, Q.; Jiang, L.; Liu, Z.; Zhang, G.; Zhang, D., New fused conjugated molecules with fused thiophene and pyran units for organic electronic materials. *RSC Advances* **2020,** *10*, 12378-12383.

(13) a) Yeung, C. S.; Dong, V. M., Catalytic dehydrogenative cross-coupling: forming carbon-carbon bonds by oxidizing two carbon-hydrogen bonds. *Chem. Rev.* **2011,** *111*, 1215-1292; b) Yamaguchi, J.; Yamaguchi, A. D.; Itami, K., C-H bond functionalization: emerging synthetic tools for natural products and pharmaceuticals. *Angew. Chem. Int. Ed.* **2012,** *51*, 8960-9009.

(14) Nakano, M.; Niimi, K.; Miyazaki, E.; Osaka, I.; Takimiya, K., Isomerically pure anthra[2,3-*b*:6,7-*b*']-difuran (*anti*-ADF), -dithiophene (*anti*-ADT), and -diselenophene (*anti*-ADS): selective synthesis, electronic structures, and application to organic field-effect transistors. *J. Org. Chem.* **2012,** *77*, 8099-8111.

(15) a) Rao, K. P.; Kondo, M.; Sakamoto, R.; Kusamoto, T.; Nishikawa, M.; Kume, S.; Nihei, M.; Oshio, H.; Nishihara, H., Benzo[e]pyrene skeleton dipyrylium dication with a strong donor-acceptor-donor interaction, and its two-electron reduced molecule. *Chem. Eur. J.* **2011,** *17*, 14010-14019; b) VanVeller, B.; Robinson, D.; Swager, T. M., Triptycene diols: a strategy for synthesizing planar π systems through catalytic conversion of a poly(*p*-phenylene ethynylene) into a poly(*p*-phenylene vinylene). *Angew. Chem. Int. Ed.* **2012,** *51*, 1182-1186.

(16) a) Wang, S.; Lv, B.; Cui, Q.; Ma, X.; Ba, X.; Xiao, J., Synthesis, Photophysics, and Self-Assembly of Furan-Embedded Heteroarenes. *Chem. Eur. J.* **2015,** *21*, 14791-14796; b) Anamimoghadam, O.; Symes, M. D.; Long, D. L.; Sproules, S.; Cronin, L.; Bucher, G., Electronically Stabilized Nonplanar Phenalenyl Radical and Its Planar Isomer. *J. Am. Chem. Soc.* **2015,** *137*, 14944-14951; c) Wehrmann, C. M.; Charlton, R. T.; Chen, M. S., A Concise Synthetic Strategy for Accessing Ambient Stable Bisphenalenyls toward Achieving Electroactive Open-Shell π-Conjugated Materials. *J. Am. Chem. Soc.* **2019,** *141*, 3240-3248.

(17) Dong, S.; Gopalakrishna, T. Y.; Han, Y.; Phan, H.; Tao, T.; Ni, Y.; Liu, G.; Chi, C., Extended Bis(anthraoxa)quinodimethanes with Nine and Ten Consecutively Fused Six-Membered Rings: Neutral Diradicaloids and Charged Diradical Dianions/Dications. *J. Am. Chem. Soc.* **2019,** *141*, 62-66.

(18) Wu, D.; Pisula, W.; Haberecht, M. C.; Feng, X.; Mullen, K., Oxygen- and sulfur-containing positively charged polycyclic aromatic hydrocarbons. *Org. Lett.* **2009,** *11*, 5686-5689.

(19) Wang, Y.; Qiu, S.; Xie, S.; Zhou, L.; Hong, Y.; Chang, J.; Wu, J.; Zeng, Z., Synthesis and Characterization of Oxygen-Embedded Quinoidal Pentacene and Nonacene. *J. Am. Chem. Soc.* **2019,** *141*, 2169-2176.

(20) a) Yin, J.; Tan, M.; Wu, D.; Jiang, R.; Li, C.; You, J., Synthesis of Phenalenyl-Fused Pyrylium Cations: Divergent C-H Activation/Annulation Reaction Sequence of Naphthalene Aldehydes with Alkynes. *Angew. Chem. Int. Ed.* **2017,** *56*, 13094-13098; b) Li, C.; Zhu, L.; Liang, W.; Su, R.; Yin, J.; Hu, Y.; Lan, Y.; Wu, D.; You, J., An unusual [4 + 2] fusion strategy to forge *meso-N/O*-heteroarene-fused (quinoidal) porphyrins with intense near-infrared Q-bands. *Chem. Sci.* **2019,** *10*, 7274-7280.

(21) a) Pummerer, R.; Prell, E.; Rieche, A., Darstellung von Binaphthylendioxyd. *Ber. Dtsch. Chem. Ges. A/B* **1926,** *59*, 2159-2161; b) Pummerer, R.; Rieche, A., Über aromatische Peroxyde und einwertigen Sauerstoff. (IX. Mitteilung) über die Oxydation der Phenole). *Ber. Dtsch. Chem. Ges. A/B* **1926,** *59*, 2161-2175.

(22) a) Đorđević, L.; Valentini, C.; Demitri, N.; Meziere, C.; Allain, M.; Salle, M.; Folli, A.; Murphy, D.; Manas-Valero, S.; Coronado, E.; Bonifazi, D., O-Doped Nanographenes: A Pyrano/Pyrylium Route Towards Semiconducting Cationic Mixed-Valence Complexes. *Angew. Chem. Int. Ed.* **2020,** *59*, 4106-4114; b) Lawrence, J.; Sosso, G. C.; Đorđević, L.; Pinfold, H.; Bonifazi, D.; Costantini, G., Combining high-resolution scanning tunnelling microscopy and first-principles simulations to identify halogen bonding. *Nat. Commun.* **2020,** *11*, 2103.

(23) a) Stassen, D.; Demitri, N.; Bonifazi, D., Extended O-Doped Polycyclic Aromatic Hydrocarbons. *Angew. Chem. Int. Ed.* **2016,** *55*, 5947-5951; b) Berezin, A.; Biot, N.; Battisti, T.; Bonifazi, D., Oxygen-Doped Zig-Zag Molecular Ribbons. *Angew. Chem. Int. Ed.* **2018,** *57*, 8942-8946.

(24) a) Miletić, T.; Fermi, A.; Orfanos, I.; Avramopoulos, A.; De Leo, F.; Demitri, N.; Bergamini, G.; Ceroni, P.; Papadopoulos, M. G.; Couris, S.; Bonifazi, D., Tailoring Colors by O Annulation of Polycyclic Aromatic Hydrocarbons. *Chem. Eur. J.* **2017,** *23*, 2363-2378; b) Sciutto, A.; Berezin, A.; Lo Cicero, M.; Miletić, T.; Stopin, A.; Bonifazi, D., Tailored Synthesis of N-Substituted *peri*-Xanthenoxanthene Diimide (PXXDI) and Monoimide (PXXMI) Scaffolds. *J. Org. Chem.* **2018,** *83*, 13787-13798; c) Sciutto, A.; Fermi, A.; Folli, A.; Battisti, T.; Beames, J. M.; Murphy, D. M.; Bonifazi, D., Customizing Photoredox Properties of PXX-based Dyes through Energy Level Rigid Shifts of Frontier Molecular Orbitals. *Chem. Eur. J.* **2018,** *24*, 4382-4389.

(25) a) Kamei, T.; Uryu, M.; Shimada, T., Cu-Catalyzed Aerobic Oxidative C-H/C-O Cyclization of 2,2'-Binaphthols: Practical Synthesis of PXX Derivatives. *Org. Lett.* **2017,** *19*, 2714-2717; b) Takaishi, K.; Hinoide, S.; Matsumoto, T.; Ema, T., Axially Chiral *peri*-Xanthenoxanthenes as a Circularly Polarized Luminophore. *J. Am. Chem. Soc.* **2019,** *141*, 11852-11857.

(26) a) Figueira-Duarte, T. M.; Mullen, K., Pyrene-based materials for organic electronics. *Chem. Rev.* **2011,** *111*, 7260-7314; b) Casas-Solvas, J. M.; Howgego, J. D.; Davis, A. P., Synthesis of substituted pyrenes by indirect methods. *Org. Biomol. Chem.* **2014,** *12*, 212-232; c) Deng, C. L.; Bard, J. P.; Zakharov, L. N.; Johnson, D. W.; Haley, M. M., PN-Containing Pyrene Derivatives: Synthesis, Structure, and Photophysical Properties. *Org. Lett.* **2019,** *21*, 6427-6431; d) Lu, Q.; Kole, G. K.; Friedrich, A.; Muller-Buschbaum, K.; Liu, Z.; Yu, X.; Marder, T. B., Comparison Study of the Site-Effect on Regioisomeric Pyridyl-Pyrene Conjugates: Synthesis, Structures, and Photophysical Properties. *J. Org. Chem.* **2020,** *85*, 4256-4266.

(27) a) Loudet, A.; Burgess, K., BODIPY dyes and their derivatives: syntheses and spectroscopic properties. *Chem. Rev.* **2007,** *107*, 4891-4932; b) Boens, N.; Verbelen, B.; Dehaen, W., Postfunctionalization of the BODIPY Core: Synthesis and Spectroscopy. *Eur. J. Org. Chem.* **2015,** *2015*, 6577-6595.

(28) a) Nowak-Król, A.; Würthner, F., Progress in the synthesis of perylene bisimide dyes. *Org. Chem. Front.* **2019,** *6*, 1272-1318; b) Würthner, F.; Saha-Moller, C. R.; Fimmel, B.; Ogi, S.; Leowanawat, P.; Schmidt, D., Perylene Bisimide Dye Assemblies as Archetype Functional Supramolecular Materials. *Chem. Rev.* **2016,** *116*, 962-1052.

(29) Crawford, A. G.; Liu, Z.; Mkhalid, I. A.; Thibault, M. H.; Schwarz, N.; Alcaraz, G.; Steffen, A.; Collings, J. C.; Batsanov, A. S.; Howard, J. A.; Marder, T. B., Synthesis of 2- and 2,7-functionalized pyrene derivatives: an application of selective C-H borylation. *Chem. Eur. J.* **2012,** *18*, 5022-5035.

(30) Mocanu, A.; Szucs, R.; Caytan, E.; Roisnel, T.; Dorcet, V.; Bouit, P. A.; Nyulaszi, L.; Hissler, M., Synthesis, Optical, and Redox Properties of Regioisomeric Benzoheterocycles-Fused Pyrene. *J. Org. Chem.* **2019,** *84*, 957-962.

(31) Zhang, S.; Qiao, X.; Chen, Y.; Wang, Y.; Edkins, R. M.; Liu, Z.; Li, H.; Fang, Q., Synthesis, structure, and opto-electronic properties of regioisomeric pyrene-thienoacenes. *Org. Lett.* **2014,** *16*, 342-345.

(32) Menges, N., Computational study on aromaticity and resonance structures of substituted BODIPY derivatives. *Comput. Theor. Chem.* **2015,** *1068*, 117-122.

(33) Chen, J.; Burghart, A.; Derecskei-Kovacs, A.; Burgess, K., 4,4-Difluoro-4-bora-3a,4a-diaza-*s*-indacene (BODIPY) dyes modified for extended conjugation and restricted bond rotations. *J. Org. Chem.* **2000,** *65*, 2900-2906.

(34) a) Nagarajan, K.; Mallia, A. R.; Reddy, V. S.; Hariharan, M., Access to Triplet Excited State in Core-Twisted Perylenediimide. *J. Phys. Chem. C* **2016,** *120*, 8443-8450; b) Nagarajan, K.; Mallia, A. R.; Muraleedharan, K.; Hariharan, M., Enhanced intersystem crossing in core-twisted aromatics. *Chem. Sci.* **2017,** *8*, 1776-1782.

(35) a) Zhao, N.; Xuan, S.; Fronczek, F. R.; Smith, K. M.; Vicente, M. G., Enhanced Hypsochromic Shifts, Quantum Yield, and π-π Interactions in a *meso*,beta-Heteroaryl-Fused BODIPY. *J. Org. Chem.* **2017,** *82*, 3880-3885; b) Farinone, M.; Cybińska, J.; Pawlicki, M., A controlled blue-shift in *meso*-nitrogen aryl fused DIPY and BODIPY skeletons. *Org. Chem. Front.* **2019,** *6*, 2825-2832.

(36) Yanai, T.; Tew, D. P.; Handy, N. C., A new hybrid exchange–correlation functional using the Coulomb-attenuating method (CAM-B3LYP). *Chem. Phys. Lett.* **2004,** *393*, 51-57.

(37) a) Chen, Z.; Wannere, C. S.; Corminboeuf, C.; Puchta, R.; Schleyer, P., Nucleus-independent chemical shifts (NICS) as an aromaticity criterion. *Chem. Rev.* **2005,** *105*, 3842-3888; b) Gershoni-Poranne, R.; Stanger, A., Magnetic criteria of aromaticity. *Chem. Soc. Rev.* **2015,** *44*, 6597-6615.